Exploration of pre-salt targets off-shore Brazil using least-squares RTM

Diego Carotti (CGG)*, Mariano Gatti (CGG) and Huub Douma (CGG)

This paper was prepared for presentation during the 15th International Congress of the Brazilian Geophysical Society held in Rio de Janeiro, Brazil, 31 July to 3 August, 2017.

Abstract

Least-squares (LS) migration attempts to invert the propagation of waves as they travel through the earth to obtain an estimate of the reflectivity. As such it goes beyond standard imaging that uses the adjoint of the modeling operator only. Therefore it promises to remove illumination variations due to both the acquisition geometry and complex overburdens. This means it has an application for the exploration of pre-salt targets in Brazil, where the reservoirs are typically buried underneath a complex overburden consisting often of a combination of volcanics, carbonates and salt. Moreover, almost all streamer acquisition off-shore Brazil has so far been narrow azimuth, and it is well known that such acquisition imposes substantial illumination variations. Here we present the application of an image-domain single iteration LS-RTM imaging to narrow-azimuth streamer data from two important basins off-shore Brazil: the Santos and Espírito Santo basins. We show that such imaging can indeed improve the amplitudes of images below a complex overburden and reduce migration artifacts, when compared to standard RTM. We validate the effectiveness of the method by calculating point-spread functions (PSFs) after LS-RTM and comparing them to PSFs after standard RTM in terms of amplitude balancing and focusing of the PSFs. We show that comparison of the PSFs resulting from both methods provides a robust approach to quality-control the result from LS-RTM, in terms of correcting for illumination variations.

Introduction

Migration of seismic data involves moving data from the location where they were recorded in the data domain to their corresponding location in the image domain. Even though the location in the image domain is accurate according to a given velocity model, this method does not compensate for amplitude variations due to illumination variations. These illumination variations originate from the used acquisition geometry as well as from the focusing and de-focusing of waves as they travel through the overburden before (and after) they hit the reflectors. Mathematically speaking, this means that the data are operated on by the adjoint of the modeling operator instead of its inverse. Therefore, after standard migration such as RTM, the image of the geological targets still contains amplitude variations due to illumination variations.

Least-squares migration (LSM) aims to invert the propagation of waves as they travel through the earth for the reflectivity, and as such promises also to remove amplitude variations in the image due to both acquisition geometry and a complex overburden, as well as increase the resolution of the imaged reflectors and reduce migration artefacts. Various methods have been proposed for LSM, some using an iterative inversion (Tarantola, 1987; Schuster, 1993; Nemeth et al., 1999) and others using a single-iteration inversion only (Hu et al., 2001; Rickett, 2003; Guitton, 2004; Lecomte, 2008; Khalil et al., 2016). Considering the computational expense of LSM, single iteration methods are preferred over iterative methods. Therefore recently, Wang *et. al* (2016), inspired by the work of Guitton (2004) and He *et. al* (2013), introduced a curvelet domain Hessian filter (CHF) to approximate LSM using a single iteration in the image domain.

Here we apply CHF to two field datasets offshore Brazil acquired using narrow-azimuth (NAZ) streamer acquisitions in the Santos and Espírito Santo basins. Because in Brazil almost all streamer acquisitions so far have been NAZ surveys, it is particularly relevant for off-shore exploration in the pre-salt to estimate the benefits of using LSM in terms of its ability to remove illumination variations due to the acquisition geometry. Considering that CHF can in principle be done using different types of migration algorithms such as Kirchhoff or reverse-time migration (RTM), we mention that we use it here only in the context of RTM. Throughout this work we shall use the terms CHF and LSRTM interchangeably, but it should always be understood that the method we use to approximate LSRTM is always CHF applied in the image domain.

Estimating the effectiveness of LSM on the images before and after application of LSM can be cumbersome as it is impossible to separate amplitude variations due to illumination variations from amplitude variations due to subsurface reflectivity variations. In order to have a measure of the effectiveness of LSM, point-spread functions can be calculated for standard RTM as well as for CHF. Knowing that in principle CHF should remove amplitude variations due to illumination variations, the amplitudes of the PSFs after application of CHF should be more uniform as a function of position inside the image, when compared to the amplitude of the PSFs after standard RTM. This can be used to quality-control the application of LSM. In this paper we show the application of this quality control for two field datasets. We emphasize that we do not use the PSFs to deconvolve the image in any way as in migration deconvolution. We

only use the PSFs resulting from CHF and standard RTM to estimate if CHF successfully rebalances the amplitudes and thus corrects for amplitude variations due to illumination variations.

Curvelet domain Hessian filtering

LSM in the image domain in essence involves the application of the inverse Hessian to a migrated image. Iterative approaches to this inversion are still expensive because they involve many migrations as well as modeling operations. To overcome this, Guitton (2004) first proposed the use of non-stationary matching filters to approximate the inverse of the Hessian matrix in a single iteration. More recently, Wang *et al.* (2016) extended this idea by estimating such a filter in the curvelet domain. The curvelet domain is preferred to the spatial domain to avoid unwanted event shifting and for its capability to better match events with different dips (e.g. reflectors close to faults or salt flanks).

In Guitton's approach we start with a reverse time migration (RTM) of the recorded data d_0 to obtain the migrated image m_0:

$$m_0 = L^T d_0 \,,$$

where L^T denotes the migration operator, i.e. the adjoint of the Born modeling operator L . Then we perform a Born modeling using the migration velocity and m_0 to obtain the synthetic data d_1. The new image m_1 is then the result of the remigration of d_1, i.e.

$$m_1 = L^T d_1 = L^T L\, m_0$$

where m_1 is the newly obtained image. The operator $L^T L$ is generally referred to as the Hessian. It is therefore clear that m_0 can be obtained from m_1 by multiplying it with the inverse Hessian. This means that an estimate of the inverse Hessian filter F can be computed by minimizing the following cost function:

$$f(F) = \frac{1}{2}\|m_0 - F m_1\| \quad \text{where} \quad F \approx (L^T L)^{-1}$$

Applying F to the migrated image m_0, we get the approximate least-squares migration image m_{LS}:

$$m_{LS} = (L^T L)^{-1} L^T d_0 \approx F m_0$$

The formulation for obtaining the Hessian filter in the curvelet domain (Wang *et al*., 2016) consists of rewriting the cost function as

$$f(s) = \|C(m_0) - sC(m_1)\|^2 + \epsilon\|s\|^2$$

where C denotes the forward curvelet transform operator, s is the matching filter, and ϵ is the Tikhonov regularization parameter. The LSM output image is then computed as:

$$m_{LS} \approx C^{-1}\big(|s| C(m_0)\big)$$

with C^{-1} the inverse curvelet transform operator. Note that we use $|s|$ to apply the filter, to make sure the used filtering is zero phase. We also mention that in principle this CHF method can be applied in both the image as well as the data domain. Throughout this work, however, we will always assume CHF is applied in the image domain.

Assessing the quality of LSM

Like any other processing step in the data-processing sequence, LSM requires accurate quality control and a careful review of the obtained results. As mentioned in the introduction, simply comparing images before and after LSM can be hampered by the variable nature of the reflectivity in the earth. To overcome this we propose to use PSFs to evaluate the effectiveness of CHF. The benefit of using PSFs is that the input reflectivity (or for point-scatterer possibly more precisely called "diffractivity") is unity by definition. Therefore, when applying the approximate inverse Hessian to the PSFs obtained from standard migration of point-diffractors, we expect the resulting amplitudes of the PSFs to be again uniformly close to unity, independent of the position of the point-scatterers in the model. In this way we can quality control the ability of LSM to indeed remove illumination variations, because there are no amplitude variations from subsurface reflectivity variations in the input reflectivity.

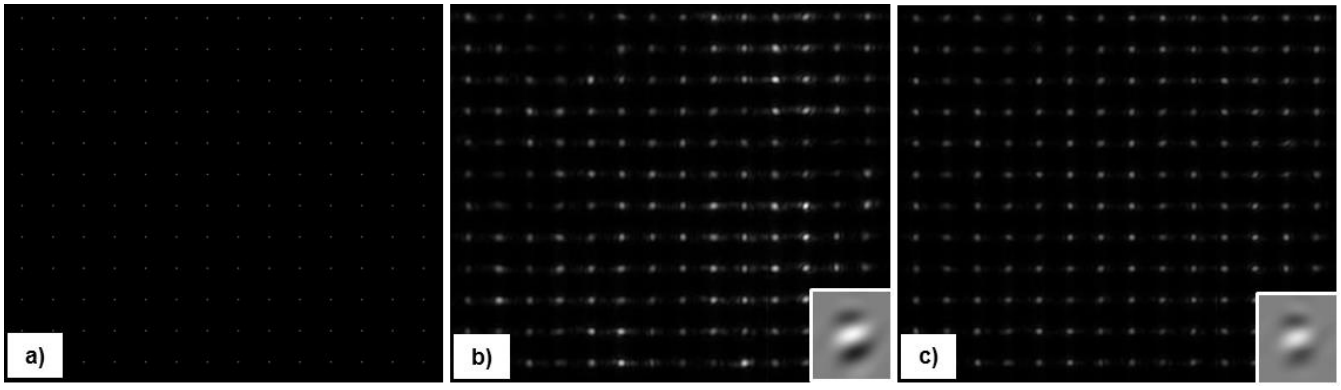

Figure 1 – *a) Input grid of point-scatterers with unit reflectivity at depth slice z=4000m (partly in the post-salt area and partly inside the salt) through an area of the Libra area in the Santos Basin, b) depth slice (same depth) through PSFs resulting from Born modeling and RTM of the point-scatterers in a), and c) depth slice (same depth) through PSFs resulting from the application of CHF to the PSFs shown in b). All images show the RMS amplitude in a window of 100m centered on depth z=4000m. The improved amplitude balancing of PSFs after CHF in c) implies that it has successfully removed most of the illumination variations. Furthermore, some improvement in the resolution of the PSFs after CHF can be observed when compared to the PSFs obtained using RTM in b). The insets in b) and c) show a vertical slice through the middle of one PSF before and after CHF.*

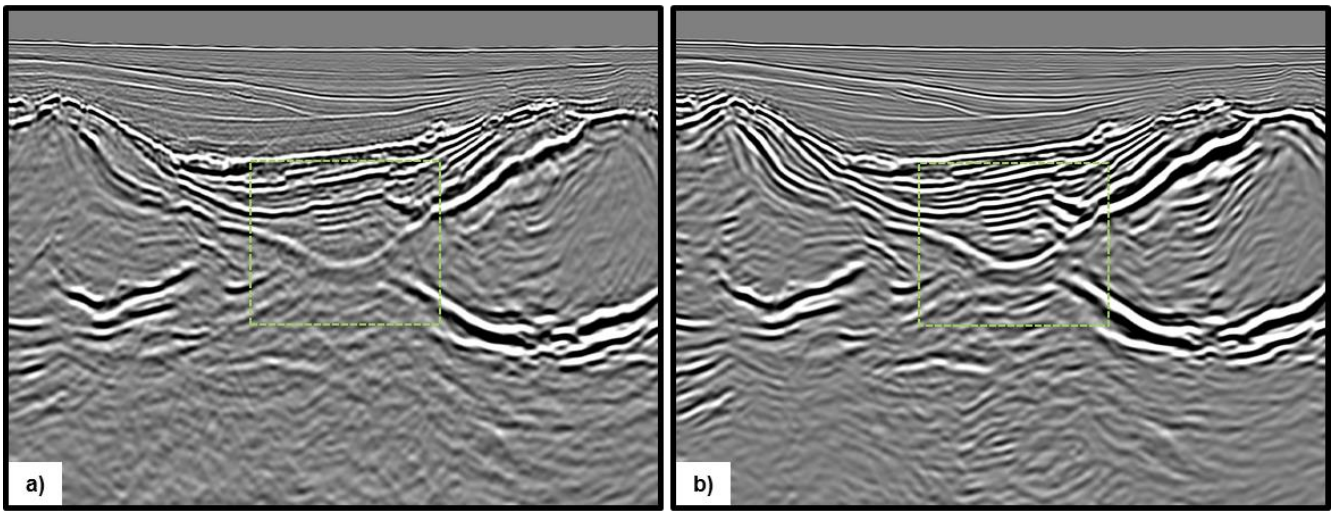

Figure 2– *a) RTM migrated inline section of the field data in the Santos basin and b) the image obtained using CHF. As anticipated from Figure 1, the amplitudes have been rebalanced in b) compared to a). Furthermore the migration artifacts visible in a) (in particular in the shallow part) have been substantially reduced and several pre-salt reflectors are showing improved lateral continuity. The green boxes indicates the areas for which a zoomed image is displayed in Figure 3 for both methods.*

To calculate the PSFs, we start with a 3D grid of point-scatterers. Using a given velocity model and the field-data acquisition geometry, we perform a Born modeling L using the grid of point-scatterers as the input reflectivity model. The resulting data are subsequently migrated to obtain the PSFs. Due to acquisition geometry effects and velocity model, as well as the bandlimited nature of the modeled data, the energy is spread away from the point-scatterer. The resulting PSFs provides an estimate of the resolution obtained from the migration for each point in the model. It is important that the separation between the point-scatterers be large enough that the PSFs will not interfere. Typically 1 to 1.5 times the local wavelength should be enough. Using the resulting PSFs from RTM as input to LSRTM, we can then gauge the effectiveness of LSRTM in removing the illumination variations due to both the acquisition geometry and the velocity model.

Figure 1a shows the input point-scatterer grid for a depth slice at z=4000m for a part of the Libra area in the Santos Basin. For this particular area, this depth is for some parts above the salt, and for some parts inside the salt. The resulting PSFs from RTM are shown in Figure 1b, showing the limited resolution obtained from RTM in focusing, bandwidth and amplitude. The illumination variations can now clearly be observed as variations in amplitude for different point-scatterer locations, as well as the variations of the shapes of the PSFs. Figure 1c shows the result of applying CHF to the PSFs from Figure 1b. The amplitudes are now more evenly distributed indicating that CHF has removed most illumination variations. Furthermore, a slight improvement in the focusing of the PSFs can be observed when compared to the RTM result (cf. Figure 1b, as well as the insets on Figures 1b and 1c highlighting the effect on in the vertical direction for one particular PSF). However, we mention that because CHF uses a matching filter approach, the slight improved focusing will be somewhat different on the field data than for the PSFs. This is due to the fact that the field data image mostly consists of a superposition of mostly curve-like bandlimited events, whereas a single PSF has more of a point-scatterer nature by design. As such the matching filter will behave slightly differently in this respect. However, the proposed method works well to assess the degree to which CHF rebalances the amplitude variations due to illumination variations.

The use of PSFs to assess the quality of LSM can first be used on a smaller target area of interest. In this way the feasibility of using LSRTM to improve the image quality compared to RTM, can be assessed prior to running a full scale production LSRTM.

Before we continue to discuss the field data results, we note once more that even though we use PSFs to quality control the application of CHF, we do not in any way use the PSFs to deconvolve the data, as done by Fletcher *et al*. (2016). The PSFs are used only to assess the quality of the resulting LSM, focusing mostly on the rebalancing of the amplitudes of the PSFs after LSM. Furthermore we remind the reader that LSM does not update the velocity model. As such, LSM is not expected to recover events that are not well imaged to begin with, due to a poor velocity model.

Results – CHF applied to the Libra area in the Santos basin

We applied the CHF method to two field datasets offshore Brazil. Both datasets have their reservoirs in the pre-salt area and both datasets were acquired with NAZ streamer acquisition geometries. The first dataset was acquired over the Libra area in the Santos basin. During acquisition, severe feathering of the cables was observed due to the strong currents in this area. As a consequence parts of the area have variable fold as well as severe illumination variations. Moreover, the well-known subsurface complexities of the overburden with a combination of carbonates, volcanics and salt provide

plenty of complexity that results in illumination variations on the image of the pre-salt reservoir. CHF was applied to an RTM image over a fully-migrated area of about 150 km^2 using a maximum frequency of 23 Hz. We computed the inverse Hessian filter in the curvelet domain using the RTM stacks as input. Here we applied CHF in the post-stack domain, but the method can also be applied in the pre-stack domain to provide offset or angle gathers. Figure 2a and b show the inline section for the RTM and CHF images, respectively. Comparing both images first in the shallow part, it is clear that the CHF image has less acquisition footprint just below the water bottom. Moreover, CHF nicely attenuates the migration artifacts in the shallow parts, as well as in the deeper parts in the salt and pre-salt area (see also Figure 3).

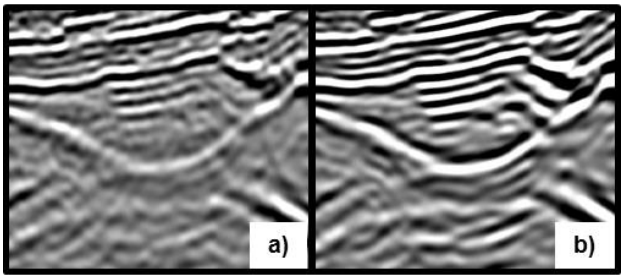

Figure 3 – *Zooms of the boxes shown on the inline migrated sections of the real data in the Santos basin in Figure 2, a) RTM and b) CHF.*

The PSF quality control was performed for both a depth window partly in the post-salt and partly inside the salt at z=4000m (see Figure 1) and for a deeper window at z=6000m in the pre-salt (see Figure 4). For both windows we observe that LSRTM corrects the illumination variations well. This provides further confidence in the amplitude balancing due to LSRTM observed in the inline stacked image shown in Figures 2b and 3b. Furthermore the PSFs after LSRTM in Figures 1c and 4b suggest some increased resolution after LSRTM for both depth windows. As mentioned previously this improvement is not so well visible on the stacked images in Figure 2b and 3b. The data are already broadband because both source- as well as receiver-side deghosting have been applied prior to CHF. Furthermore we mention that we used a source-wavelet with a flat spectrum for the modeling and re-migration to calculate m_1 and that no attenuation compensation was used.

Results – CHF for field data in the Espírito Santo basin

Our second field data example is from a BroadSeis NAZ streamer acquisition acquired in 2014 in the Espírito Santo basin. During acquisition the cables did not feather as much as in the previous Libra field data case, so the data were more regular. However, in this basin the presence of huge allochthonous salt bodies in the subsurface causes substantial illumination variations and therefore hampers the imaging of the pre-salt reservoirs. Figure 5 shows the comparison between two inline migrated stacks from a pre-salt area using both RTM (a) and CHF (b). The migration artifacts have been substantially reduced by the application of CHF, and the amplitudes have been rebalanced as expected. The PSFs before and after application of CHF (see Figure 6) confirm that CHF substantially reduces the illumination variations. In this case the quality control using the PSFs was done

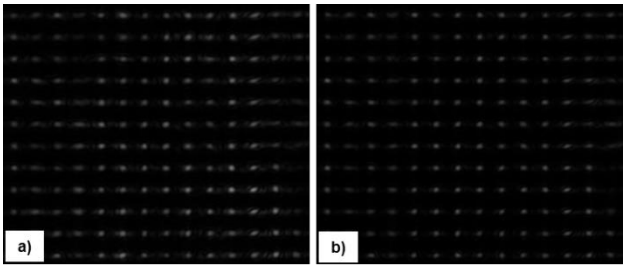

Figure 4 – *a) PSFs resulting from Born modeling and RTM of point-scatterers at a depth of z=6000m (in the pre-salt) through an area of the Libra area in the Santos Basin, and b) PSFs resulting from the application of CHF to the PSFs shown in a). All images show the RMS amplitude in a window of 100m centered on depth z=6000m. The amplitudes of the PSFs are more balanced after CHF and we observe some small improvement in the resolution of the PSFs after CHF.*

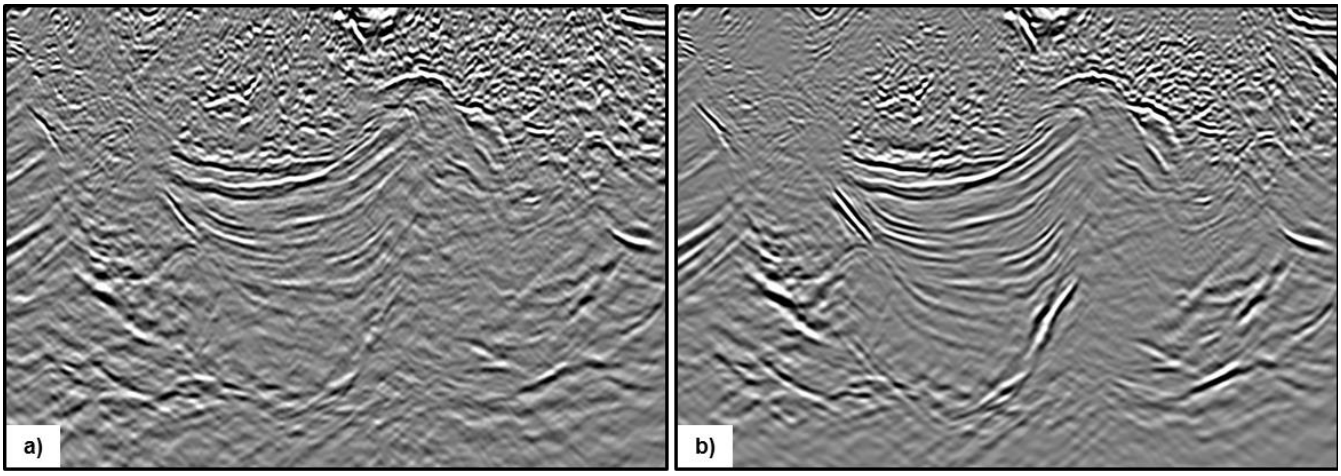

Figure 5 – *a) RTM migrated inline section of the field data in the Espírito Santo basin and b) the image obtained using CHF. Migration artifacts are substantially reduced and amplitudes have been rebalanced due to the correction for illumination variations resulting from CHF. As a result the spatial continuity of amplitudes along several pre-salt reflectors has been improved.*

on a smaller part of the area, prior to full-scale application of CHF to the field data, in order to verify if the illumination variations would be substantially removed. In that way processing of the field data using CHF was justified.

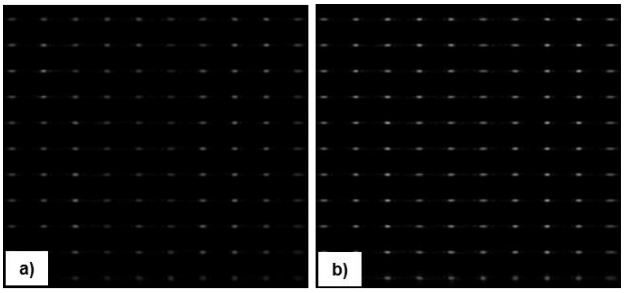

Figure 6 – *a) PSFs resulting from Born modeling and RTM of point-scatterers at a depth of z=6000m (in the pre-salt) through an area in the Espírito Santo basin, and b) PSFs resulting from the application of CHF to the PSFs shown in a). All images show the RMS amplitude in a window of 100m centered on depth z=6000m. The amplitudes of the PSFs are clearly more balanced after CHF.*

Conclusions

We showed the application of a curvelet domain Hessian filter (CHF) to approximate LSRTM using a single iteration in the image domain, to two NAZ streamer field datasets in both the Santos and the Espírito Santo basins offshore Brazil. For both field data sets, the targets are in the pre-salt which is buried underneath a complex overburden. For each of these datasets we observe that CHF attenuates migration artefacts well when compared to standard RTM. Moreover CHF substantially reduces the amplitude variations due to illumination variations. As a result we see improved continuity along pre-salt reflectors for both data sets. LSRTM therefore benefits the exploration of pre-salt targets offshore Brazil. Furthermore, we found that comparison of PSFs resulting from RTM and LSRTM allows to isolate amplitude variations due to illumination variations from amplitude variations due to subsurface reflectivity variations. It provides a reliable quality control (QC) to verify the extent to which LSRTM is able to correct for amplitude variations due to illumination variations. This QC can be done on a smaller target area of interest prior to application to the field data, to justify full-scale computationally expensive application of LSRTM.

Acknowledgments

We thank the Libra consortium and CGG Multi-Client New-Ventures for the permission to show the field data examples. We also thank CGG for permission to publish this work and our colleagues around the world for several fruitful discussions.

References

FLETCHER, R. P., D. NICHOLS, R. BLOOR, & R. T. COATES, 2016, Least-squares migration — Data domain versus image domain using point spread functions: The Leading Edge, 35, 157–162,

GUITTON, A., 2004, Amplitude and kinematic corrections of migrated images for nonunitary imaging operators: Geophysics, 69, 1017–1024,

HE, K., J. SUN & X. TANG, 2013, Guided image filtering: IEEE Transactions on Pattern Analysis and Machine Intelligence, 35, 1397–1409,

HU, J., G. T. SCHUSTER & P. A. VALASEK, 2001, Poststack migration deconvolution: Geophysics, 66, 939–952,

KHALIL, A., H. HOEBER, G. ROBERTS & F. PERRONE, 2016. An alternative to least-squares imaging using data-domain matching filters: 86th Annual International Meeting, SEG, Expanded Abstracts, 4188-4192.

LECOMTE, I., 2008, Resolution and illumination analyses in PSDM: A ray-based approach: The Leading Edge, 27, 650–663,.

NEMETH, T., C. WU, & G. T. SCHUSTER, 1999, Least-squares migration of incomplete reflection data: Geophysics, 64, 208–221,

RICKETT, J. E., 2003, Illumination-based normalization for wave equation depth migration: Geophysics, 68,1371–1379,

SCHUSTER, G. T., 1993, Least-squares crosswell migration: 63rd Annual International Meeting, SEG, Expanded Abstracts, 110–113,

TARANTOLA, A., 1987, Inverse problem theory: Methods for data fitting and model parameter estimation: Elsevier Science Publishing Company.

WANG, P., A. GOMES, Z. ZHANG & M. WANG, 2016. Least-squares RTM: Reality and possibilities for subsalt imaging: 86th Annual International Meeting, SEG, Expanded Abstracts, 4204–4209,